



EULER-CALCULATION OF THE FLOW FIELD AROUND A HELICOPTER ROTOR
IN FORWARD FLIGHT

BY

R. STANGL AND S. WAGNER

INSTITUT FÜR AERODYNAMIK UND GASDYNAMIK
UNIVERSITÄT STUTTGART, GERMANY

TWENTIETH EUROPEAN ROTORCRAFT FORUM
OCTOBER 4 - 7, 1994 AMSTERDAM

Euler-Calculation of the Flow Field Around a Helicopter Rotor in Forward Flight

R. Stangl
S. Wagner
Institut für Aerodynamik und Gasdynamik
Universität Stuttgart

Abstract

An existing implicit 3-D Eulercode for the calculation of the flow field around a helicopter rotor in hover has been extended for calculations of a rotor in forward flight. Comparisons of the solutions with measurements for nonlifting testcases were carried out and demonstrated good agreement. Calculations were also done for lifting forward flight with pitching, lagging and flapping. Special attention was given to 'wake capturing', the proper conservation of the wake and tip vortex structure. In addition, the method is able to calculate the impulsive noise characteristics of the main rotor.

Notation

A, B, C	Jacobi matrices of the Fluxes
D	Determinante of the inverse Jacobi matrix
E, F, G	Flux vectors
I	Identity matrix
K	Right-hand side vector
R	Rotor radius
S	Jacobian of K
$\bar{U}, \bar{V}, \bar{W}$	contravariant, absolute velocities
$-c_p$	Local pressure coefficient
\bar{e}	Total energy per unit volume
p	Pressure
r	Radius
u, v, w	Velocities in x, y, z direction
\bar{u}, \bar{v}	Absolute velocities
x, y, z	Kartesian coordinates
$\dot{x}, \dot{y}, \dot{z}$	Grid velocity in x,y,z direction
Φ	Solution vector
ρ	Density
ξ, η, ζ	Curvilinear coordinates
ω	Angular velocity of the coordinate frame

1. Introduction

The calculation of a flow field around a helicopter demands high standards on the numerical method, which is due to the combined presence of complex flow phenomena. The optimum program which satisfies every requirement is beyond current computer capacities. However, it is possible to gain meaningful results with methods that can be developed for existing high speed computers.

The most significant component of a helicopter is the main rotor. Here the flow is characterized by a wide velocity range which starts at a very low Mach number (and even reversed flow) and goes up to the transonic speed range.

Viscous effects dominate the flow on the retreating blade, with its low velocities and high angles of attack.

On the advancing blade transonic effects have the dominant influence. In high speed forward flight strong shocks can appear near the blade tip, which generate a strong acoustic pattern and emit the high-speed-impulsive noise.

The change of the velocity happens very rapid. The blade is exposed to extremal values during a tenth of a second. This leads to intensive unsteady effects like hysteresis in the aerodynamic coefficients, dynamic stall on the retreating blade and shock movement on the advancing blade. These are intensified by the blade motion, in particular the pitch, flap and lag motion.

One major characteristic of helicopter aerodynamics is the wake. In contrast to fixed wing configurations, it usually remains longer near the blades and can influence the flow field drastically, especially at low or zero advance ratios. It interacts with the following blades, with the fuselage and the tail rotor and has a significant influence on the acoustic behaviour, on vibrations and on the performance of certain flight conditions.

External requirements lead to fuselage shapes which are not optimized for drag reduction. Flow separation occurs, due to the complex configuration with engine inlets and outlets, short wings and external loads.

In addition the tailrotor complicates the flow field. Strong interactions with the main rotor and the fuselage appear which have influence on vibrations and noise.

The industry is highly interested in predicting the complete flow field, the loads on rotor, fuselage and tail rotor, the aeroelastic behaviour of the blades and the emission of noise. In addition a tool for an efficient design of single components and complete configurations is needed.

An optimum computer code has to fulfill many contradicting requirements. The complex geometry demands advanced grid generation. The code must handle components with relative motion. Important effects take place far away from the surfaces, this requires dense grids. The method used must conserve the wake and pressure pulses over a long distance in order to calculate the loads on the blade and the acoustic field correctly. The proper prediction of transonic and viscous effects is essential. And above all the code has to be fast and flexible to allow an economical conceptual design.

Because all these requirements can not be met at a time, we have to make some simplifications. The geometry in the present stage is reduced to the main rotor. The extension to calculations with the fuselage is currently in developement. We use an Euler code instead of a Navier-Stokes method, therefore we are limited to nonviscous flows. But the wake and the pressure pulses are preserved over a wide range and transonic effects are well represented. The advantage compared to a Navier-Stokes method is the lower requirement of computer resources.

In the present stage we are able to calculate the following flight conditions: hover, non-lifting forward flight, lifting forward flight with wake capturing but without arbitrary blade motion, lifting forward flight with arbitrary blade motion but without wake capturing. In addition the acoustic field can be predicted.

2. Baseline solution algorithm

Governing Equations :

In accordance with the flow field of the rotor, the compressible Euler equations are formulated within a blade-attached kartesian coordinate system which rotates with the angular velocity ω of the rotor. Thus the important centrifugal and Coriolis forces are considered. Hence, the Euler equations can be written in a differential formulation with time dependent boundary conditions

$$\bar{\Phi}_t + \bar{E}_\xi + \bar{F}_\eta + \bar{G}_\zeta = \bar{K} \quad (1)$$

with the solution vector

$$\Phi = D(\rho, \rho\bar{u}, \rho\bar{v}, \rho\bar{w}, \bar{e})^T \quad (2)$$

the spatial fluxes

$$\bar{E} = \begin{pmatrix} \rho[\bar{U} + \omega(y\bar{\xi}_x - x\bar{\xi}_y)] \\ \rho\bar{u}[\bar{U} + \omega(y\bar{\xi}_x - x\bar{\xi}_y)] + p\bar{\xi}_x \\ \rho\bar{v}[\bar{U} + \omega(y\bar{\xi}_x - x\bar{\xi}_y)] + p\bar{\xi}_y \\ \rho\bar{w}[\bar{U} + \omega(y\bar{\xi}_x - x\bar{\xi}_y)] + p\bar{\xi}_z \\ \bar{e}[\bar{U} + \omega(y\bar{\xi}_x - x\bar{\xi}_y)] + p\bar{U} - p\bar{\xi}_x \end{pmatrix} \quad (3 a)$$

$$\bar{F} = \begin{pmatrix} \rho[\bar{V} + \omega(y\bar{\eta}_x - x\bar{\eta}_y)] \\ \rho\bar{u}[\bar{V} + \omega(y\bar{\eta}_x - x\bar{\eta}_y)] + p\bar{\eta}_x \\ \rho\bar{v}[\bar{V} + \omega(y\bar{\eta}_x - x\bar{\eta}_y)] + p\bar{\eta}_y \\ \rho\bar{w}[\bar{V} + \omega(y\bar{\eta}_x - x\bar{\eta}_y)] + p\bar{\eta}_z \\ \bar{e}[\bar{V} + \omega(y\bar{\eta}_x - x\bar{\eta}_y)] + p\bar{V} - p\bar{\eta}_x \end{pmatrix} \quad (3 b)$$

$$\bar{G} = \begin{pmatrix} \rho[\bar{W} + \omega(y\bar{\zeta}_x - x\bar{\zeta}_y)] \\ \rho\bar{u}[\bar{W} + \omega(y\bar{\zeta}_x - x\bar{\zeta}_y)] + p\bar{\zeta}_x \\ \rho\bar{v}[\bar{W} + \omega(y\bar{\zeta}_x - x\bar{\zeta}_y)] + p\bar{\zeta}_y \\ \rho\bar{w}[\bar{W} + \omega(y\bar{\zeta}_x - x\bar{\zeta}_y)] + p\bar{\zeta}_z \\ \bar{e}[\bar{W} + \omega(y\bar{\zeta}_x - x\bar{\zeta}_y)] + p\bar{W} - p\bar{\zeta}_x \end{pmatrix} \quad (3 c)$$

and the right-hand-side vector K

$$K = \rho\omega \cdot \begin{pmatrix} 0 \\ \bar{v} + \dot{y} \\ -\bar{u} - \dot{x} \\ 0 \\ \bar{u}\dot{y} - \bar{v}\dot{x} \end{pmatrix} \quad \bar{K} = D \cdot K \quad (4)$$

The vector K contains terms of the differentiation within the kartesian coordinate system and the centrifugal and Coriolis forces acting upon the control volumina due to the included velocities

Further definitions

$$\bar{U} = (\bar{u} - \dot{u})\bar{\xi}_x + (\bar{v} - \dot{v})\bar{\xi}_y + (w - \dot{w})\bar{\xi}_z \quad (5 a)$$

$$\bar{V} = (\bar{u} - \dot{u})\bar{\eta}_x + (\bar{v} - \dot{v})\bar{\eta}_y + (w - \dot{w})\bar{\eta}_z \quad (5 b)$$

$$\bar{W} = (\bar{u} - \dot{u})\bar{\zeta}_x + (\bar{v} - \dot{v})\bar{\zeta}_y + (w - \dot{w})\bar{\zeta}_z \quad (5 c)$$

and $u = \bar{u} + \omega y \quad v = \bar{v} - \omega x \quad \bar{e} = e - \rho\omega(\bar{u}y - \bar{v}x) - \rho/2(\omega r)^2$

Numerical Solution Algorithm :

The original numerical algorithm of the procedure was developed by Eberle [1]. On the basis of this method a completely new code was derived for the computation of the rotor flow field by Krämer, Hertel and Wagner [2,3,4,5]. It is a Godunov type algorithm, which solves the 1-D Riemann problem by an upwind scheme in each spatial direction in a grid conform coordinate system. The code is third order accurate in space and is switched to first order at shocks.

Time Accurate, Implicit Algorithm :

For time accurate calculations it is impractical to use an explicit method due to the time step restrictions. We have decided to implement an iterative relaxation scheme, namely the point Gauss-Seidel relaxation algorithm [6, 7], which is first order accurate in time.

The time derivative in equation (1) is expanded by a Taylor series. The equation is transformed to curvilinear coordinates and higher order terms are truncated. Hence, equation (1) becomes

$$\frac{\Phi^{n+1} - \Phi^n}{\Delta\tau} + E_\xi + F_\eta + G_\zeta = K \quad (6)$$

In an implicit formulation, where the fluxes are evaluated at time level n+1 equation (6) becomes

$$\frac{\Phi^{n+1} - \Phi^n}{\Delta\tau} + E_\xi^{n+1} + F_\eta^{n+1} + G_\zeta^{n+1} = K^{n+1} \quad (7)$$

The nonlinear flux vectors are expanded into a Taylor series with respect to time

$$E^{\mu+1} = E^{\mu} + \left. \frac{\partial E}{\partial \Phi} \right|^{\mu} (\Phi^{\mu+1} - \Phi^{\mu}) + O(\Delta\tau^2) + \dots \quad (8 \text{ a})$$

$$F^{\mu+1} = F^{\mu} + \left. \frac{\partial F}{\partial \Phi} \right|^{\mu} (\Phi^{\mu+1} - \Phi^{\mu}) + O(\Delta\tau^2) + \dots \quad (8 \text{ b})$$

$$G^{\mu+1} = G^{\mu} + \left. \frac{\partial G}{\partial \Phi} \right|^{\mu} (\Phi^{\mu+1} - \Phi^{\mu}) + O(\Delta\tau^2) + \dots \quad (8 \text{ c})$$

Defining the Jacobian matrices

$$A^{\mu} = \left. \frac{\partial E}{\partial \Phi} \right|^{\mu} \quad B^{\mu} = \left. \frac{\partial F}{\partial \Phi} \right|^{\mu} \quad (9)$$

$$C^{\mu} = \left. \frac{\partial G}{\partial \Phi} \right|^{\mu} \quad S^{\mu} = \left. \frac{\partial K}{\partial \Phi} \right|^{\mu}$$

and the backward differencing of the solution vector

$$\Delta\Phi^{n+1} = \Phi^{n+1} - \Phi^n \quad (10)$$

equation (7) leads to

$$\left(\frac{I}{\Delta\tau} + A_{\xi}^{\mu} + B_{\eta}^{\mu} + C_{\zeta}^{\mu} - S^n \right) \Delta\Phi^{n+1} = \text{RHS} \quad (11)$$

with the right hand side

$$\text{RHS} = - \left[\frac{\Phi^{\mu} - \Phi^n}{\Delta\tau} + E_{\xi}^{\mu} + F_{\eta}^{\mu} + G_{\zeta}^{\mu} - K \right] \quad (12)$$

Assuming that the spatial differences of the solution vector can be described by a linear function built with the values of the neighbouring cells, one has to solve formally the linear equation system

$$\overline{\overline{A}} \cdot \overline{\overline{b}} = \overline{\overline{x}} \quad (13)$$

where A is a n×n matrix (number of grid cells × number of dependent variables). Equation (13) is solved by the point Gauss-Seidel relaxation algorithm.

Boundary Conditions :

The tangency boundary condition is used at the blade surface. The fluxes through the blade surface are equal to zero. At the far field a nonreflecting boundary condition was implemented. A detailed description is given by Krämer [2].

3. Grid system

The requirement on grid generation for rotor aerodynamics are :

- the handling of complex bodies with relative motion which is the case of a complete rotorcraft configuration.
- a relative simple grid generation if only the main rotor is computed.
- a grid point distribution on the blade surface that provides a good resolution of the transonic effects.
- a dense grid even in regions far away from the blade, to cover the tip vortex and wake structure.
- a far field boundary that is some rotor lengths away in order to prevent influences from the far field on the blade.
- a grid structure that take into account the rotating reference system.
- Considering a multi-bladed rotor it is not necessary to discretize the whole rotor. A symmetric plane allows a computation with one rotor blade. With this method it is not possible to include arbitrary blade motion with a stiff mesh.

The calculations presented in this paper are performed with an O-O type grid. It has the following structure :

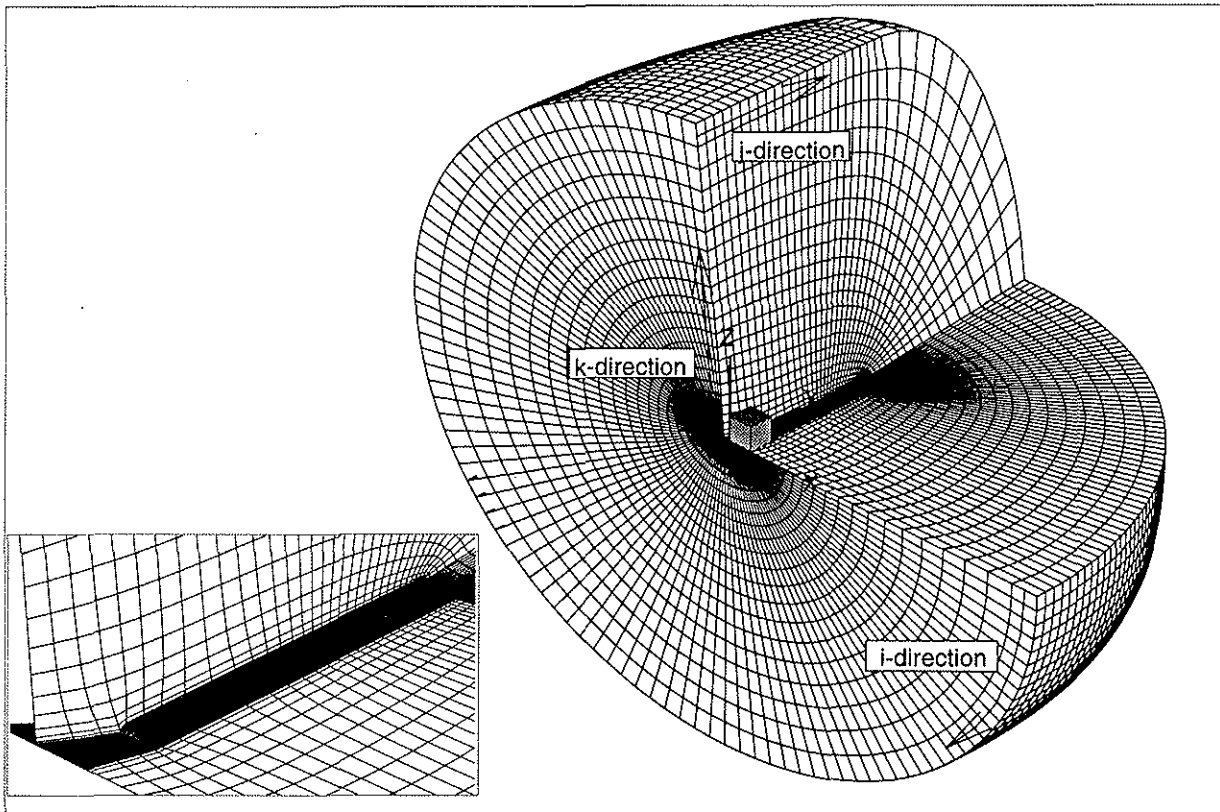


figure 1 O-O type grid

The grid parameter of the calculated test cases [8,9,10,11] are shown in Table 1.

Testcase	i-planes	number of j-planes	k-planes	number of cells	x-max	y-max	z-max
NASA model rotor	128	35	25	104.448	15.0	15.0	12.0
Bell UH-1 rotor	128	47	26	147.200	36.0	36.0	15.0

Table 1

4. Numerical results and verification

Computations are performed for the two bladed NASA model helicopter rotor and the Bell UH-1 rotor [8,9,10,11]. Table 2 shows the parameter of these rotors.

Testcase	profile	aspect ratio	begin of blade at	θ_{tip}	twist θ_v
NASA model rotor	NACA 0012	6.00	1.00 x chord	0°	0°
Bell UH-1 rotor	NACA 0012	13.78	1.34 x chord	1°	-11.11°

Table 2

4.1. Nonlifting Forward Flight

In this chapter the flow field results around the NASA model are presented and compared with experimental results of Caradonna, Laub and Tung [9]. The test case has a tip Mach number $Ma_{tip}=0.8$, an advance ratio $\mu=0.2$ and a collective pitch angle $\theta_c=0^\circ$.

The time step chosen for the calculations was equivalent to $\Delta\psi=0.3125^\circ$ of rotor revolution.

A calculation for the whole rotor half-plane from $\psi=0^\circ$ to $\psi=180^\circ$ requires approximately 8 h of CPU time on a Cray 2. It should be noted that only a small amount of investigations were made to increase the convergence rate of the code.

In figure 2 one can see the pressure coefficients on a radius station of $r/R=0.89$. Our results show good agreement with experimental data.

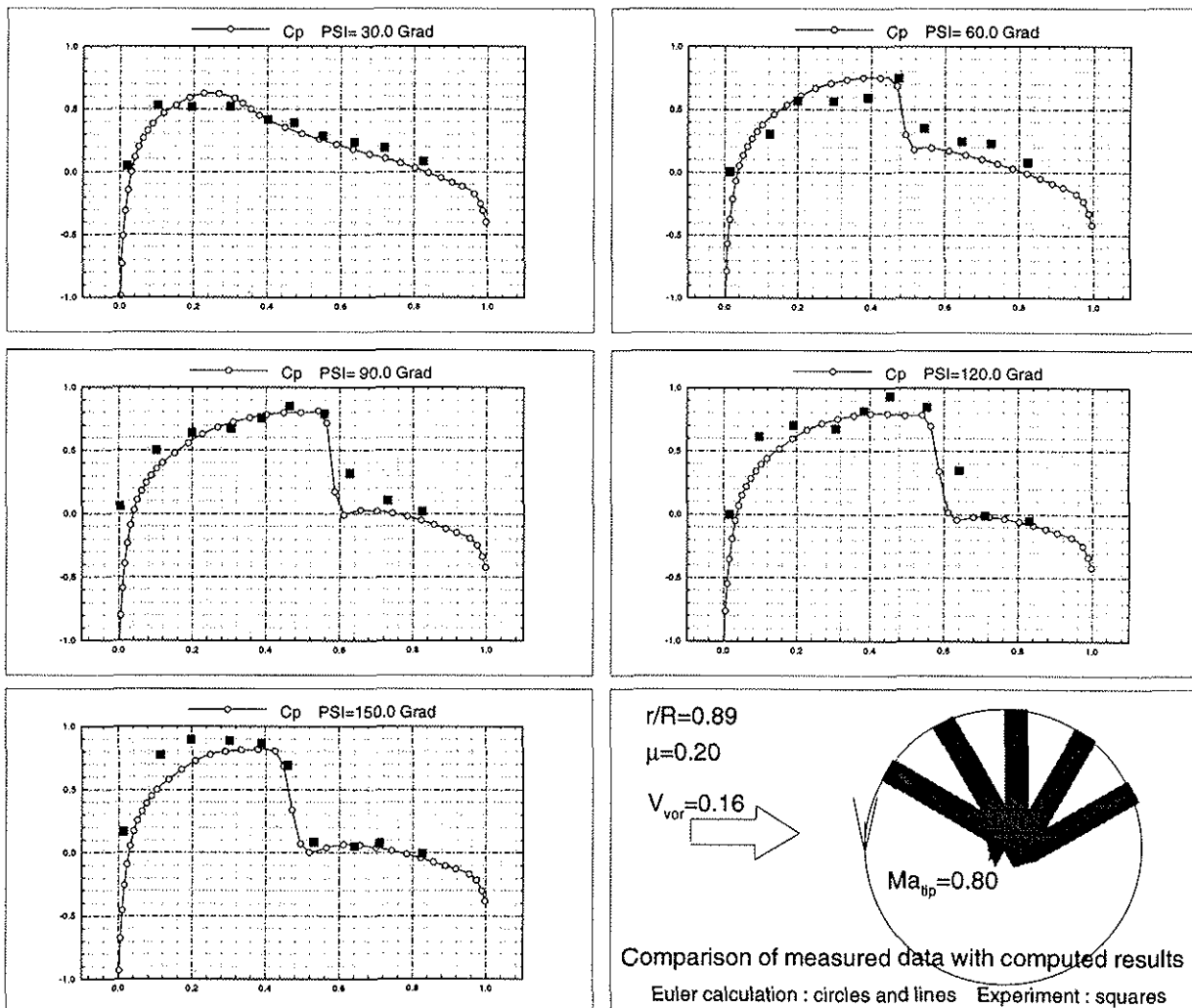


figure 2 Comparison of computed results with experimental data

In figure 3 the time history of $-c_p$ at the same radial station is presented. With this way of presentation the shock movement can be observed.

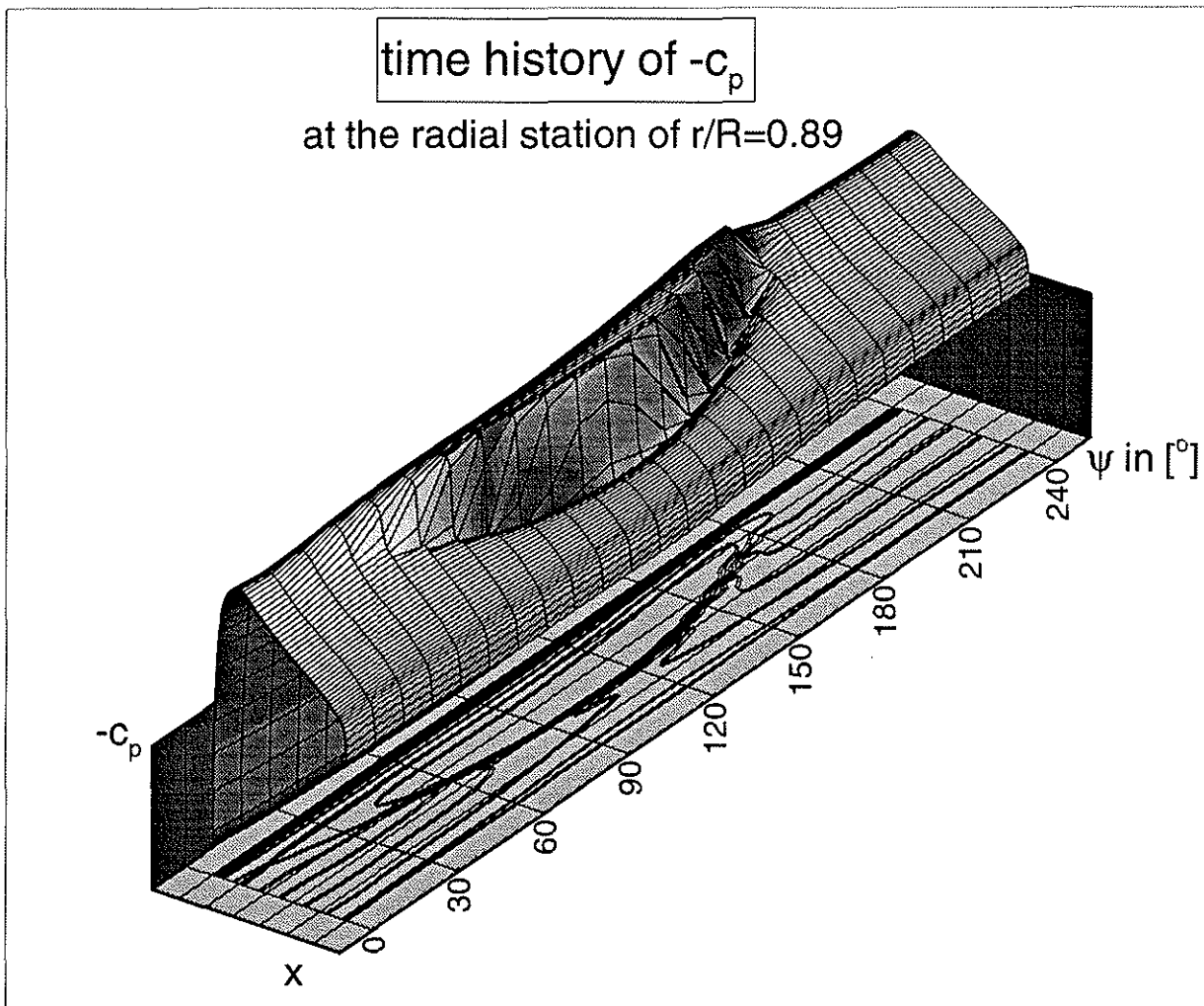


figure 3 Time history of $-c_p$

4.2. Arbitrary Blade Motion

In this chapter some results of calculations with arbitrary blade motion are presented. As mentioned above it is not yet possible to combine arbitrary blade motion with wake capturing. Therefore the influence of the preceding blade is not included.

As a reference, figure 4 shows the results of the run CASE 1 with a constant collective pitch angle $\theta_c=3^\circ$. The tip Mach number was $Ma_{tip}=0.8$ and the advance ratio $\mu=0.2$.

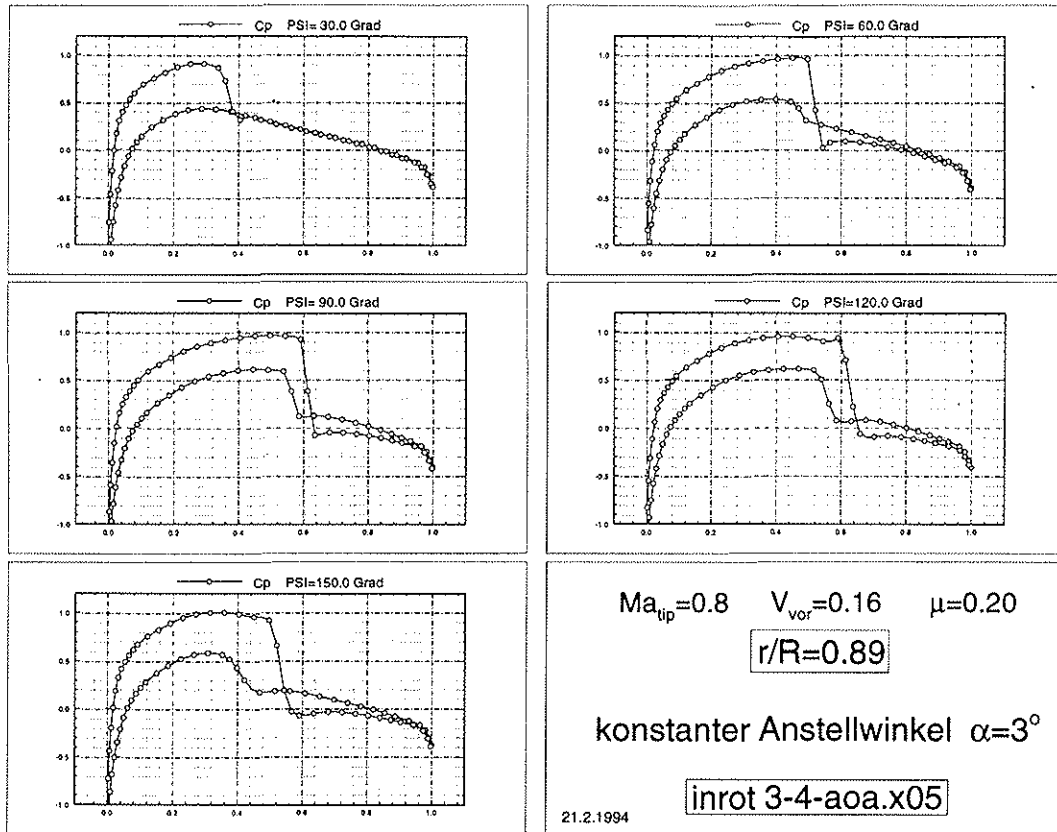


figure 4 CASE 1

In figure 5 the results of a calculation with a cyclic pitch angle are shown (CASE 2). The equation for the pitch angle was :

$$\theta_c = 3^\circ - 2^\circ \cdot \sin \psi \quad (\text{see also figure 7})$$

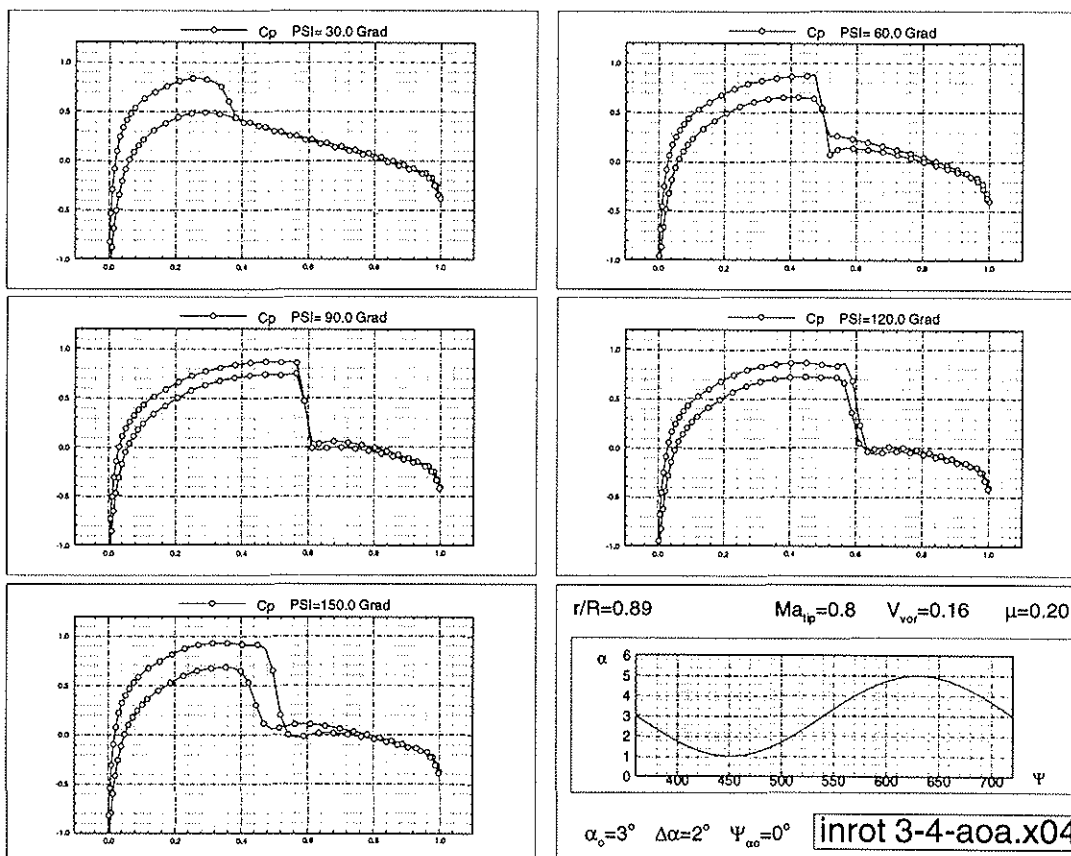


figure 5 CASE 2

In figure 6 results are shown where a flap angle was added (CASE 3). The equation for this angle was

$$\beta = 6^\circ - 6^\circ \cdot \cos\psi - 2^\circ \cdot \sin\psi \quad (\text{see also figure 7})$$

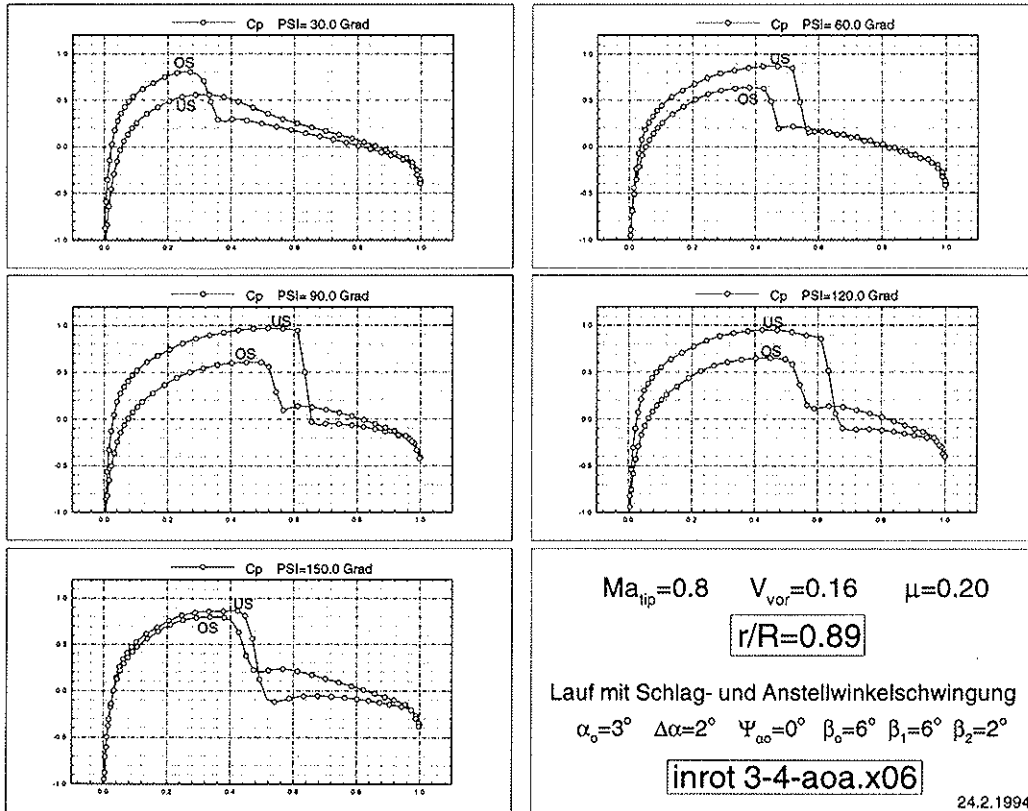


figure 6 CASE 3

To find the limits of the method, we computed an extreme test case (CASE 4) with the following blade motions (see also figure 7) :

$$\begin{aligned} \text{cyclic pitch} & \quad \theta = 3^\circ - 2^\circ \cdot \sin\psi \\ \text{flap angle} & \quad \beta = 12^\circ - 18^\circ \cdot \cos\psi - 3^\circ \cdot \sin\psi \\ \text{lag angle} & \quad \zeta = -4^\circ \cdot \cos\psi + 3^\circ \cdot \sin\psi \end{aligned}$$

Even with these extremal angles no numerical problems occurred and the results were physically correct.

Figure 7 shows the pitch, flap and lag angles for the different testcases.

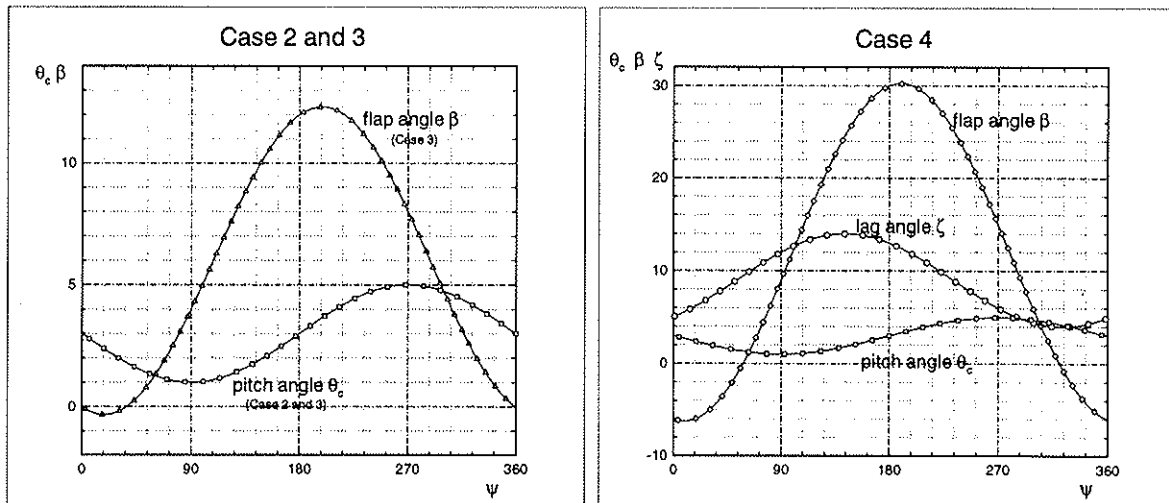


Figure 7 Pitch, flap and lag angles for the different test cases

4.3. Wake Capturing

An important requirement for proper simulation of the helicopter rotor flow is the conservation of the rotor wake. If this demand is not fulfilled an external wake model must be included [12]. For steady calculations we demonstrated that our method is able to conserve the wake correctly [2,3,4,5]. 'Wake capturing' requires a method with the following characteristics. First, the computational domain must be closed. This is fulfilled with a symmetrical plane, where the outgoing flow of one half-plane becomes the incoming flow of the other. For forward flight calculations this leads to the demand of storing the transfer values for each time step. This requires huge storage capacities. Second, the physical domain must be large enough to prevent any kind of limitation in the vortex/wake movement due to far field boundary influences.

A comparison of calculations with and without wake influence of the foregoing blade is carried out in figure 8. The z-coordinate is the difference of the pressure coefficients. For $\psi=30^\circ$ the blade is completely covered in the wake of the foregoing blade. At $\psi=50^\circ$ the tip begins to leave the wake. From $\psi=70^\circ$ to $\psi=130^\circ$ the blade escapes completely. One can observe that the difference increases near the root. This effect results from the changing angle between the blade and the tip vortex.

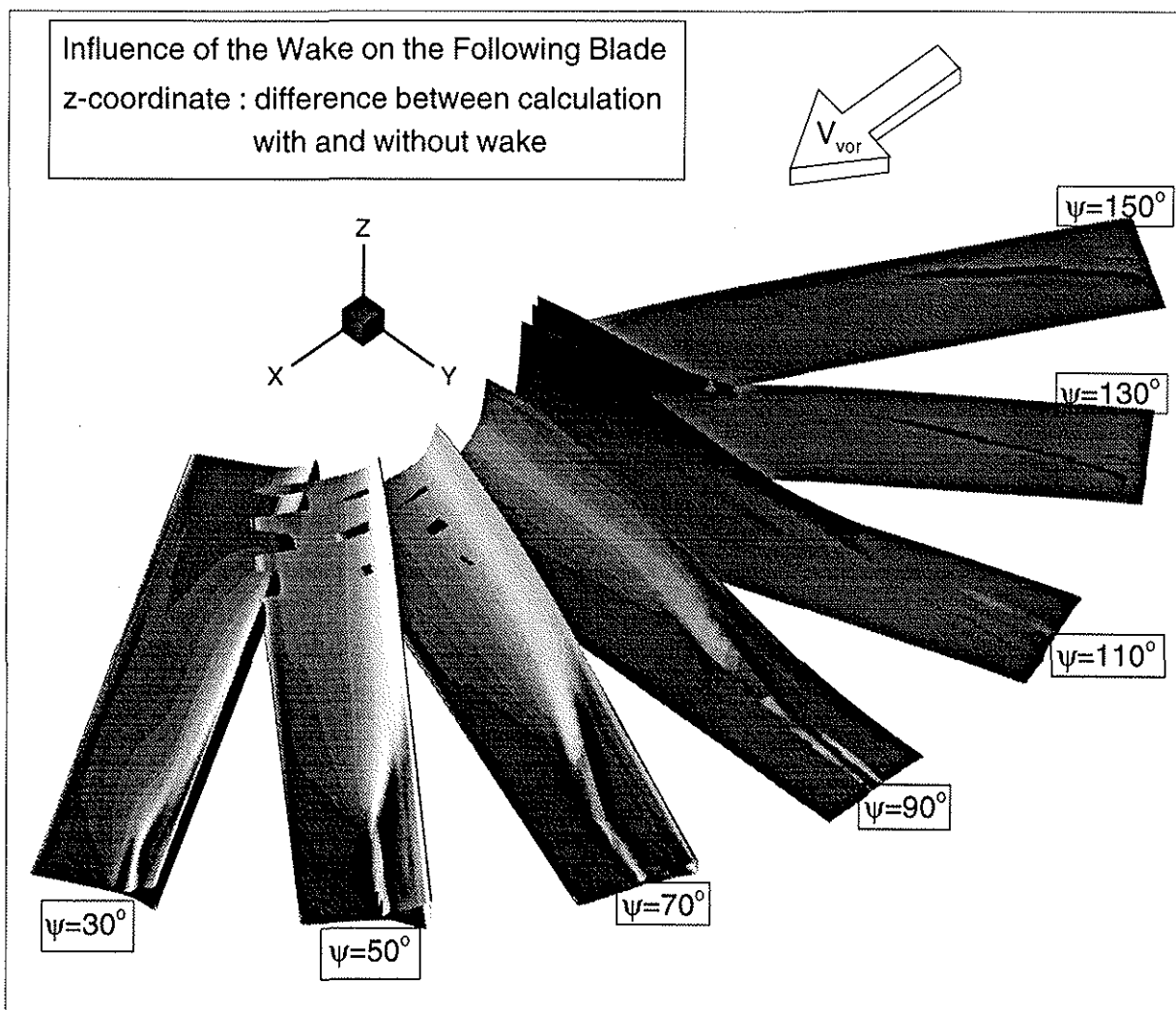


figure 8 Influence of the wake on the following blade

In figure 9 the wake is visualized for different rotor positions. The value that indicates the wake is the total pressure loss. The relative position between the blade and the wake is clearly presented.

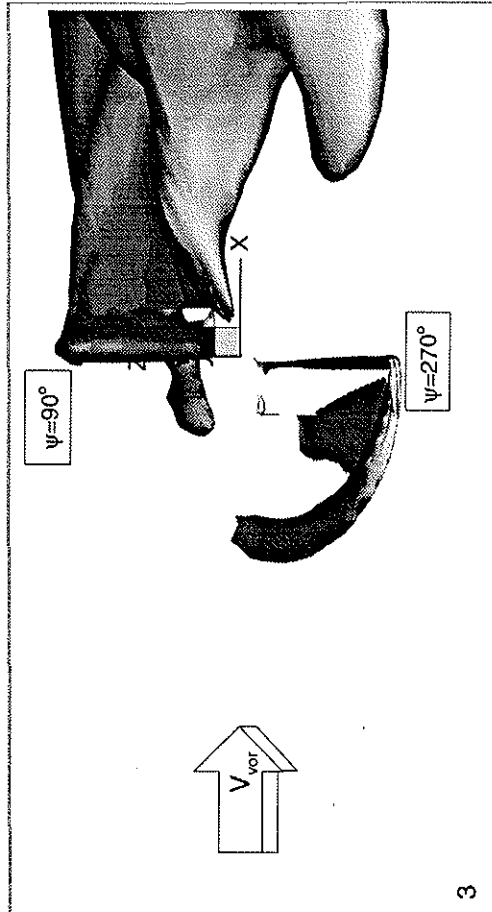
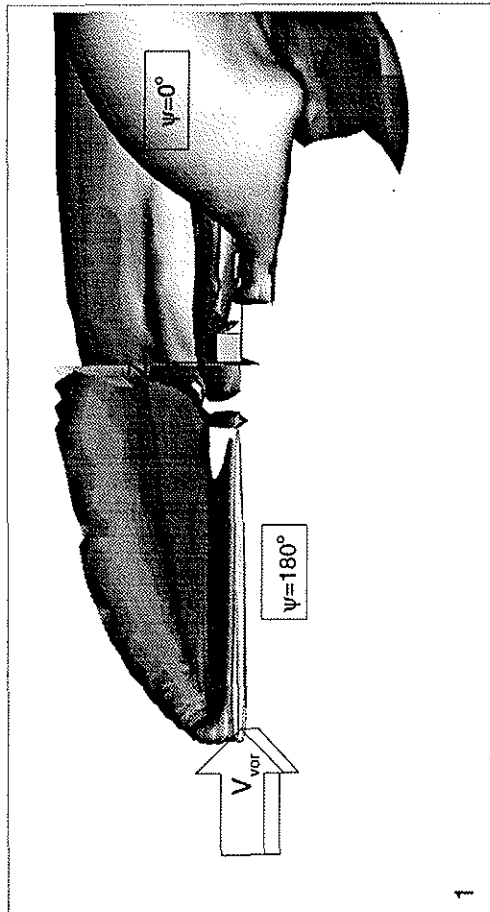
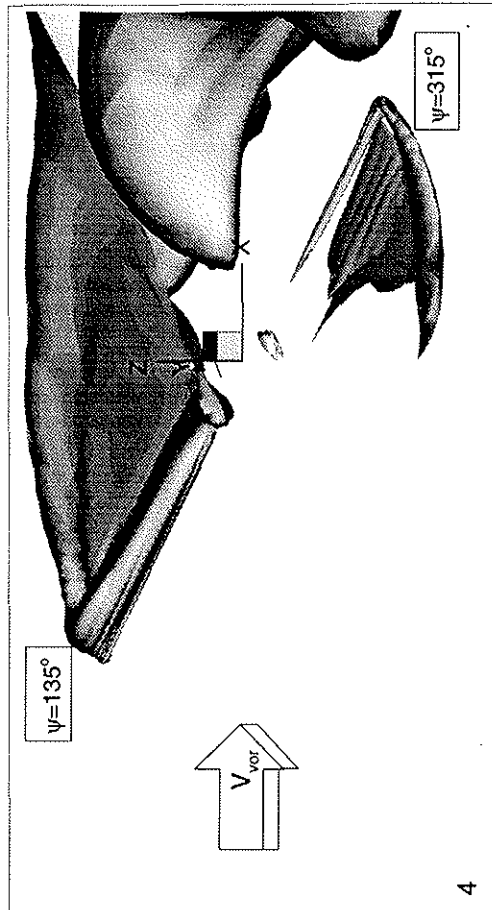
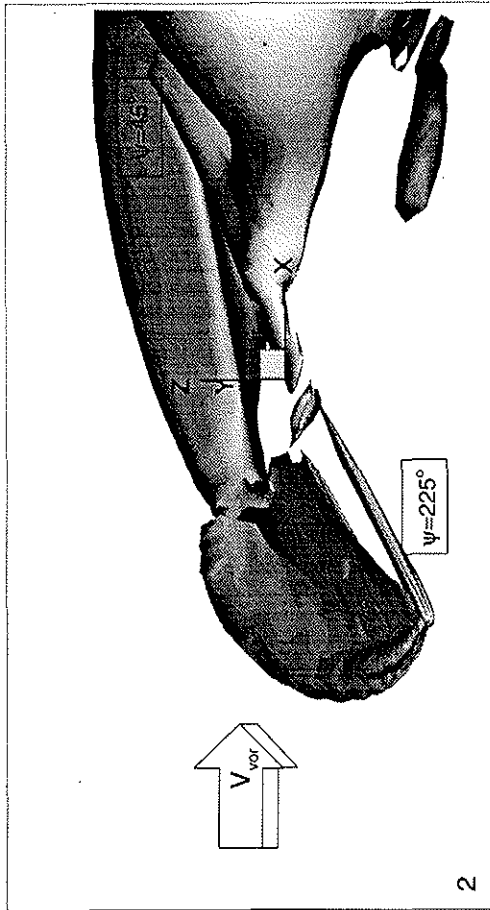


figure 9 Wake structure

5. Outlook

Further research will deal with arbitrary blade motion combined with wake capturing. Two different approaches will be examined.

First the conventional way, generating a new grid at every time step. Problems occurring with this methods are : The cell volume must be included in the governing equations, the time consumption increases drastically and the blade motion will be limited, due to grid twisting.

A second approach, which is more promising, is the utilization of overlaid embedded grids. This technique has proven its capabilities for steady rotor calculations [13]. Application of this technique to unsteady calculations are currently under development [14]. The results are very promising. We have the intention to calculate a complete rotorcraft configurations with the main rotor, the fuselage, external loads and the tail rotor in the future.

First calculations are performed to gain acoustic data with our program. The preliminary results are excellent. In the figures 10 and 11 the acoustic data of a Bell UH-1 rotor are presented. Figure 10 shows the time history of pressure pulses at certain positions relative to the blade.

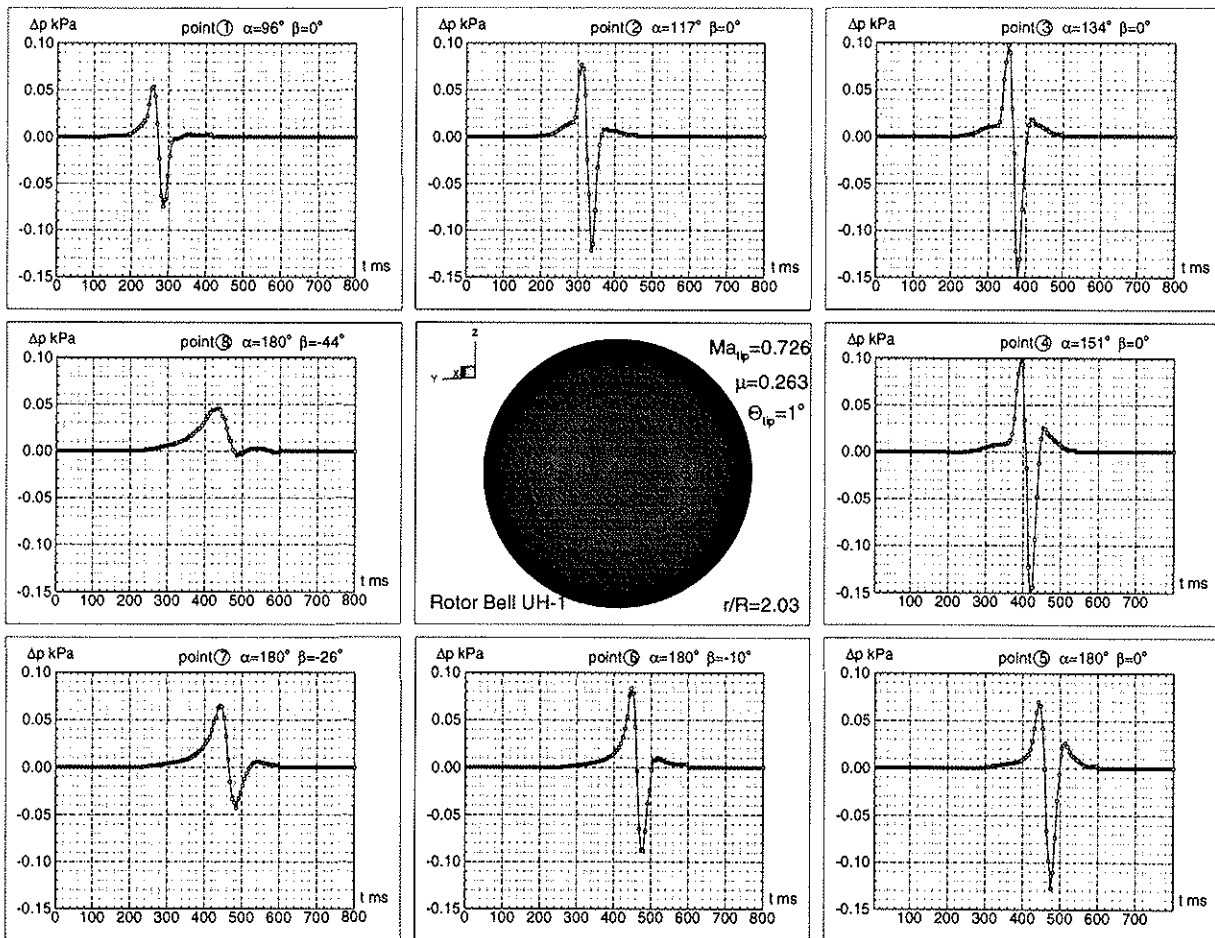


figure 10 Time history of pressure pulses

Figure 11 shows the directivities of the high speed impulsive noise.

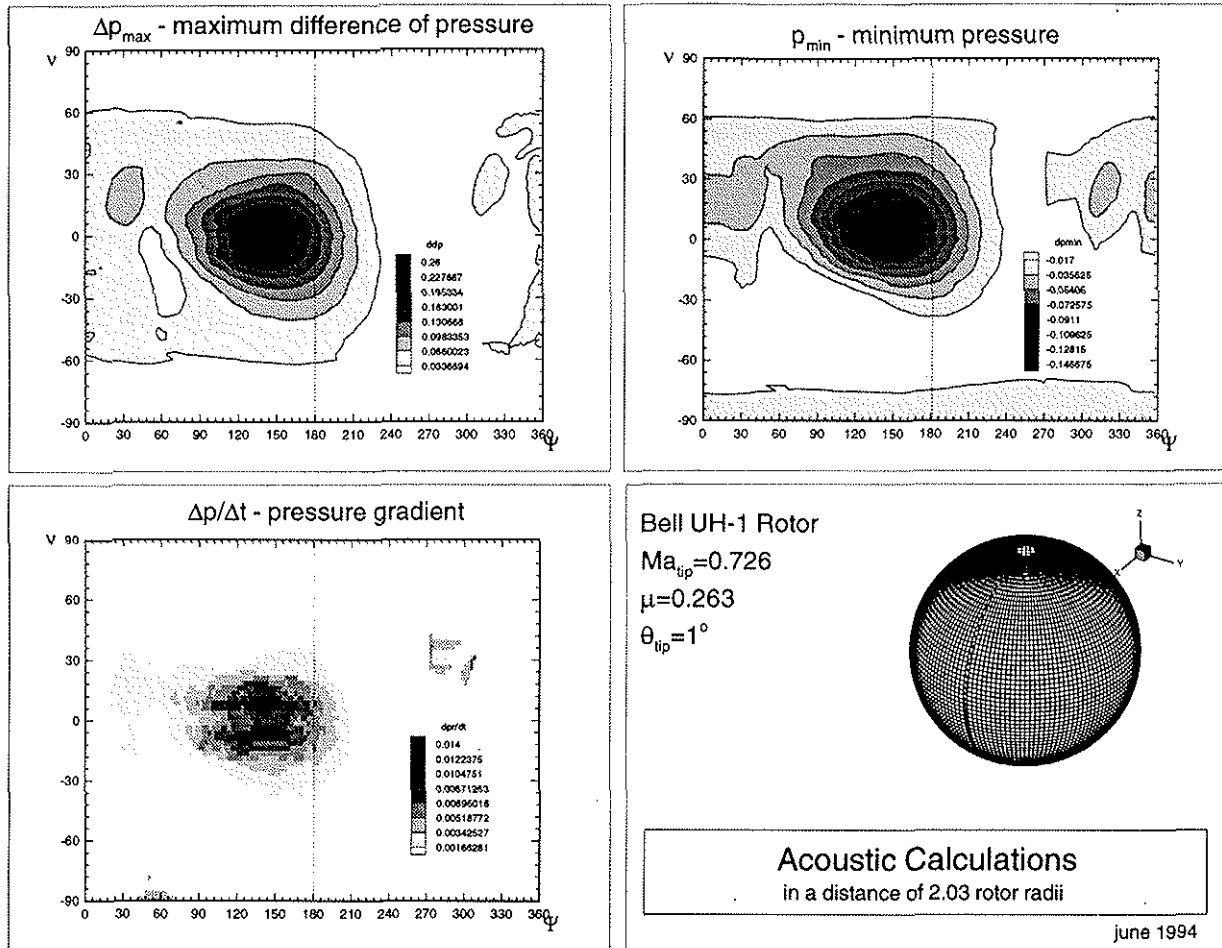


figure 11 Directivity of high-speed-impulsive noise

To improve the numerical simulation of the helicopter flow field the coupling of different methods like free-wake methods, field-panel methods, Euler methods and Navier-Stokes methods will be investigated.

Our final goal is a complete and flexible program system for the determination of the helicopter aerodynamics, aeroacoustics and aeroelastics behaviour.

6. References

- [1] A. Eberle. MBB-EUFLEX. *A New Flux Extrapolation Scheme Solving the Euler Equations for Arbitrary 3-D Geometry and Speed*. Bericht MBB/LKE122/S/PUB/140, MBB, 1984.
- [2] E. Krämer. *Theoretische Untersuchungen der stationären Rotorblattumströmung mit Hilfe eines Euler-Verfahrens*. Universität der Bundeswehr München, Dissertation an der Fakultät für Luft- und Raumfahrttechnik, 1991.
- [3] J. Hertel. *Euler-Lösungen der stationären Rotorströmung für Schweb- und den axialen Vorwärtsflug mit Einbeziehung linearer Methoden*. Universität der Bundeswehr München, Dissertation an der Fakultät für Luft- und Raumfahrttechnik, 1991.

- [4] J. Hertel, E. Krämer und S. Wagner. *Complete Euler Solution for a Rotor in Hover and a Propeller in Forward Flight*. Paper Presented at the 16th European Rotorcraft Forum, Glasgow, Scotland, 18.-21. September 1990, Proceedings, Paper No. 2.6.
- [5] E. Krämer, J. Hertel and S. Wagner. *Euler procedure for calculation of the steady rotor flow with emphasis on wake evolution*. In AIAA, 8th Applied Aerodynamics Conference, Portland, OR, Aug. 1990.
- [6] A. Brenneis. *Berechnungen instationärer zwei- und dreidimensionaler Strömungen um Tragflügel mittels eines impliziten Relaxationsverfahrens zur Lösung der Eulergleichungen*. Universität der Bundeswehr München, Dissertation an der Fakultät für Luft- und Raumfahrt-technik, 1989.
- [7] R. Stangl und S. Wagner. *Implementation of a Time Implicit Algorithm for Steady Calculations with Euler Equations*. Progress report of the BRITE/EURAM Project DACRO, Januar 1991
- [8] F.X. Caradonna, A. Desopper and C. Tung. *Finite-Difference Modeling of Rotor Flow Including Wake Effects*. Paper presented at the 8th European Rotorcraft Forum, Aix-en-Provence, France. Aug. 1982.
- [9] F.X. Caradonna, G. H. Laub and C. Tung. *An Experimental Investigation of the Parallel Blade-Vortex Interaction*. NASA TM-86005, Nov. 1984.
- [10] F. H. Schmitz and D. A. Boxwell. *In-Flight Far-Field Measurements of Helicopter Impulsive Noise* . Presented at the 32nd Annual Forum of the American Helicopter Society, May, 1976.
- [11] J. D. Ballard, K. L. Orloff and A. B. Luebs. *Effekt of Tip Shape on Blade Loading Characteristics for a Two-Bladed Rotor in Hover* . Presented at the 35nd Annual Forum of the American Helicopter Society, May, 1979.
- [12] R. K. Agarwal and J. E. Deese., *An Euler Solver for Calculating the Flowfield of a Helicopter Rotor in Hover and Forward Flight*, AIAA Paper 87-1427, Jun. 8-10, 1987.
- [13] R. Stangl und S. Wagner. *Calculation of the Steady Rotor Flow using an Overlapping-Embedded Grid Technique*. Paper presented at the 18. European Rotorcraft Forum, Avignon, France, September 1992, Proceedings, Paper No.78. 1992
- [14] D. Wehr, R. Stangl and S. Wagner. *Interpolation Schemes for Intergrid Boundary Value Transfer applied to Unsteady Transonic Flow Computations on Overlaid Embedded Grids*. Paper presented at the ECCOMAS-Conference, Stuttgart, Germany, September 1994, Proceedings, 1994